Climatic context and ecological implications of summer fog decline in the coast redwood region

James A. Johnstone[a,1] and Todd E. Dawson[a,b]

[a]Department of Environmental Science, Policy, and Management, and [b]Department of Integrative Biology, University of California, Berkeley, CA 94720

Communicated by Inez Y. Fung, University of California, Berkeley, CA, January 7, 2010 (received for review August 10, 2009)

Biogeographical, physiological, and paleoecological evidence suggests that the coast redwood [*Sequoia sempervirens* (D. Don) Endl.] is closely associated with the presence of summer marine fog along the Pacific coast of California. Here we present a novel record of summer fog frequency in the coast redwood region upon the basis of direct hourly measurements of cloud ceiling heights from 1951 to 2008. Our analysis shows that coastal summer fog frequency is a remarkably integrative measure of United States Pacific coastal climate, with strong statistical connections to the wind-driven upwelling system of the California Current and the broad ocean temperature pattern known as the Pacific Decadal Oscillation. By using a long-term index of daily maximum land temperatures, we infer a 33% reduction in fog frequency since the early 20th century. We present tree physiological data suggesting that coast redwood and other ecosystems along the United States west coast may be increasingly drought stressed under a summer climate of reduced fog frequency and greater evaporative demand.

California Current | clouds | Pacific Decadal Oscillation | *Sequoia sempervirens* | temperature inversion

The world's eastern ocean boundaries are climatically distinctive zones, sharing characteristic marine and terrestrial ecosystem traits. These regions lie under the influence of the subtropical anticyclones, which produce alongshore equatorward winds, driving ocean upwelling through offshore Ekman transport of surface waters. The delivery of cool, nutrient-rich water to the ocean surface from beneath provides the basis for productive marine ecosystems (1). In the overlying atmosphere, large-scale subsidence inhibits precipitation and maintains a capping low-level temperature inversion, separating the cool, humid marine boundary layer from warm, dry, descending air above. Synoptic conditions in these areas are conducive to the development of low-level stratocumulus clouds, which form just below the inversion base, typically several hundred meters above the sea surface (2, 3). The advection of marine stratus over land profoundly moderates the coastal terrestrial climate by reducing insolation and temperatures, raising humidity, and supplying water directly to the landscape (4–12). The last effect is particularly notable along the active tectonic margin defining the Pacific coast of the Americas, where uplifted relief intercepts marine air and cloud moisture and blocks its inland penetration. Terrestrial ecosystems in these coastal cloud-inundated areas enjoy an exotic humid climate within otherwise dry regional surroundings (6, 9, 13, 14).

Perhaps the most famous example of a cloud-connected coastal ecosystem is that of the iconic coast redwood [*Sequoia sempervirens* (D. Don) Endl.], whose natural distribution is restricted to a narrow (~50 km) belt from ~42°N to 36°N along the NE Pacific rim. The coast redwood is the tallest living tree species and notably long-lived, with some individuals exceeding 2,000 yr in age (15). *S. sempervirens* is one of three relict species recognized as redwoods that once inhabited broader areas of the Northern Hemisphere (16). Today each extant species occupies a narrow geographic range and a correspondingly small climatic envelope.

The modern coast redwood distribution, limited to the California Current upwelling zone, suggests a reliance on cool, humid marine conditions. Quaternary pollen evidence shows severe reductions in redwood populations during glacial periods (17, 18) when coastal upwelling may have been reduced (19, 20). Today, alluvial flats in west-draining canyons provide the prime habitat for the oldest and tallest redwood trees, and significant populations also occupy low-elevation coastal hillslopes and ridgetops. Redwoods are watered primarily by winter rains that residually drain through steep coastal watersheds during nearly rainless summer months.

Cloud presence produces strong effects on both the water relations (5, 21) and carbon balance (21) of the coast redwood. On hourly to daily time scales, cloud moisture within the canopy virtually eliminates the atmospheric water vapor pressure deficit, causing transpiration and sap flow to halt and, in some cases, reverse direction (5). Redwoods are poor regulators of their own water use, transpiring significant quantities of water at night when no photosynthetic benefits are gained by leaving stomata open to the atmosphere (5). This behavior highlights redwood sensitivity to ambient humidity and, consequently, the presence or absence of clouds. In coastally exposed sites, the marine stratus also provides significant quantities of water to coastal California forests (4, 7, 9, 10, 22) and grasslands (13), obtained primarily by drip from the canopy to the root zone (6) and to a lesser extent by direct foliar uptake (5, 23). Intraannual variations in δ^{18}O and δ^{13}C of redwood tree rings show significant correlations to summer low-cloud frequency over recent years (24), reflecting an integrated effect on redwood physiology.

Summer Climate of the NE Pacific and Northern California. The summer climatic setting of the NE Pacific is illustrated in Fig. 1. The North Pacific High is the dominant atmospheric feature (Fig. 1*A*), contributing to a sea-land pressure gradient that drives persistent north-northwesterly winds over the coastal ocean (25). Northerly advection and upwelling push coastal sea-surface isotherms southward, producing temperatures ~4 °C lower than at comparable latitudes in the open Pacific. On land, a strong contrast is also evident in daily maximum near-surface temperatures (T_{MAX}), which differ by nearly 20 °C between coastal and inland locations (Fig. 1*B* and *D*). Over the northern California coast, the inversion base typically occurs at elevations of 400–500 m (Fig. 1*C*), considerably lower than the prevailing topography of the Coast Ranges (Fig. 1*D*). Inland penetration of marine air is thus limited to a low-elevation coastal zone with an interior boundary defined by the inversion height and the local relief (Fig. 1*D* and *G*).

Results

Fog and Pacific Climate Variability. California marine stratus and fog have been studied primarily on daily time scales (3, 26–29) with aims toward forecasting for aviation and maritime activities.

Author contributions: J.A.J. and T.E.D. designed research; J.A.J. performed research; J.A.J. analyzed data; and J.A.J. and T.E.D. wrote the paper.

The authors declare no conflict of interest.

Freely available online through the PNAS open access option.

[1]To whom correspondence should be addressed. E-mail: jajstone@berkeley.edu.

This article contains supporting information online at www.pnas.org/cgi/content/full/0915062107/DCSupplemental.

GEOPHYSICS
ECOLOGY

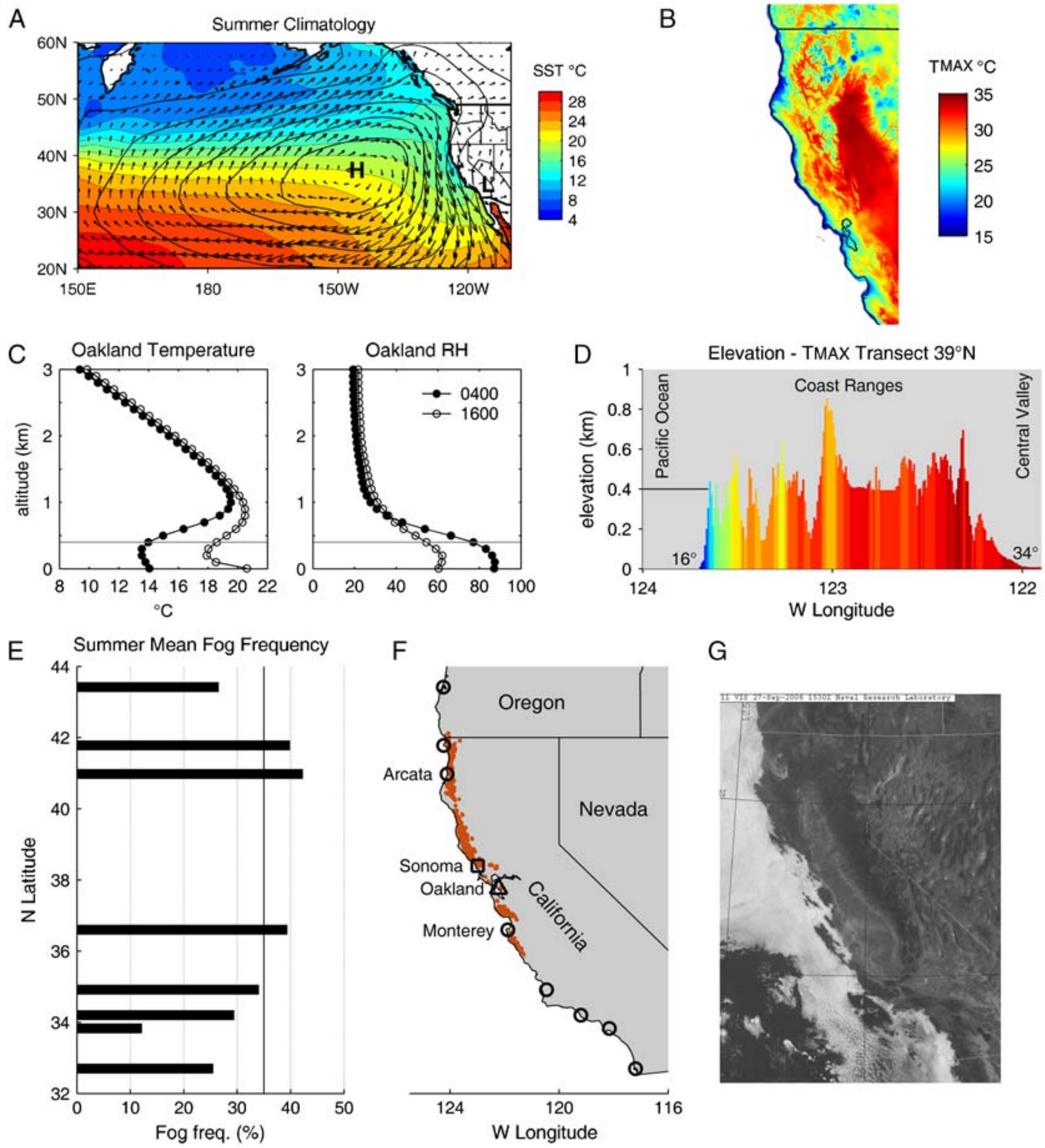

Fig. 1. Summer climatology of the NE Pacific and northern California. (*A*) Color shading: SST. Contours: SLP. Vectors: 1000 hPa wind. (*B*) Northern California summer mean T_{MAX}. (*C*) Summer mean vertical profiles of Oakland, CA temperature (*Left*) and relative humidity (*Right*). Early morning (0400 Pacific standard time) and late afternoon (1600) profiles are indicated by filled and shaded markers, respectively. Horizontal lines mark the 400 m level. (*D*) Elevation-T_{MAX} profile along 39 °N. Elevation is plotted along the *y* axis; color scale matches the map above. 400 m level is marked by a horizontal line. (*E*) Summer mean fog frequency, U.S. west coast. (*F*) Sites used in the study. Circles: Long-term cloud height measurements. Triangle: Oakland upper-air observations. Square: Sonoma field site and airport cloud height observations. Coast redwood range shaded in orange. (*G*) Visible GOES satellite image September 27, 2006, 1530 UTC.

Variability on interannual and longer scales has been examined with ship observations and surface visibility data, reflecting conditions near sea level; see, e.g., refs. 30 and 31. Low summer clouds in coastal California often reside above the sea surface, however, escaping direct measurement at low-elevation sites. In order to capture a more complete picture of ecologically relevant cloud variability (12), we used hourly records of cloud ceiling height, measured routinely at airports for operational use (see *Materials and Methods*). We focus on the frequency of cloud base heights occurring at or below 400 m elevation, which, following prior work (3), we define as fog.

Summer mean fog frequency values are illustrated for ten Pacific coast stations with at least 25 yr of observations (Fig. 1*E* and *F*). Fog frequency is greatest (40–44%) in northern and central California and declines below 30% toward Oregon and southern California. The latitudinal limits of the coast redwood distribution correspond approximately to the 35% fog threshold at both northern and southern ecotones. This result supports the long-suspected relationship between coastal fog frequency and the modern coast redwood distribution.

Historical fog variability was estimated from a pair of northern California stations with thorough records back to 1951. Summer (June–September) averages of fog frequency were calculated for airports at Arcata (40.98°N, 124.11°W, 64 m) and Monterey, CA (36.58°N, 121.85°W, 50 m), which lie near the northern and southern ends of the coast redwood range (Fig. 1*F*). Hourly summer averages indicate that nighttime fog is approximately twice as common as its daytime occurrence (Fig. S1). Seasonally, fog frequency reaches a maximum in early August, with greatest occurrence from June through September (Fig. S2). Interannual series from Arcata and Monterey are strongly correlated ($r = 0.74$) and display a stable relationship over time (Fig. 2*A*), suggesting the importance of common synoptic-scale climate forcing. To assess regional interannual variability, both records were consolidated into a single northern California fog frequency series covering summers from 1951 through 2008.

This fog record reveals substantial year-to-year changes since the mid-20th century (Fig. 2*A*). From 1951 to 1975, fog frequency varied around a mean of 44%, followed by a gradual decline through the 1980s and 1990s culminating in a record minimum of 27% in 1997. The past decade has seen a partial recovery to pre-1977 levels with an average frequency of 42%. The 1951–2008 record has a marginally insignificant ($p = 0.06$) linear trend of −0.9% per decade (−2.2% per decade in relative terms).

Examining summers of extreme anomalies, we find that fog was present 62% of the time in 1951, a frequency 2.3 times greater than the 1997 minimum (Fig. 2*A* and *B*). Sea-level pressure (SLP) patterns for each summer reveal a difference in the spatial structure of the North Pacific High (Fig. 2*C*). Northerly 1,000 hPa (near-surface) winds off the coast of Oregon (45°N, 125°W) during each summer were also the most extreme within the modern record (see *SI Text*). The summer of 1951 featured anomalous NE-ward expansion of the anticyclone and northerly winds exceeding 150% of normal (4.8 ms^{-1}). On daily time scales, the encroachment of subtropical high pressure and increased subsidence over the NW United States (U.S.) typically initiate fog development by intensifying the temperature inversion and compressing the marine layer (3, 26, 28). The persistence of similar conditions over the course of the 1951 summer can largely account for the unusually high frequency of fog. In 1997, below-average pressure prevailed off the Oregon coast, while northerly winds averaged only 1.5 ms^{-1}, less than 50% of normal. The daily evolution of fog frequency during each extreme summer (Fig. 2*B*) reveals a marked contrast in the character of its recurrence, a difference particularly strong during the day. From 1000 to 2100 hours local time, the summer of 1951 was fog-free only 13 of 122 days, compared to 62 fogless days in 1997.

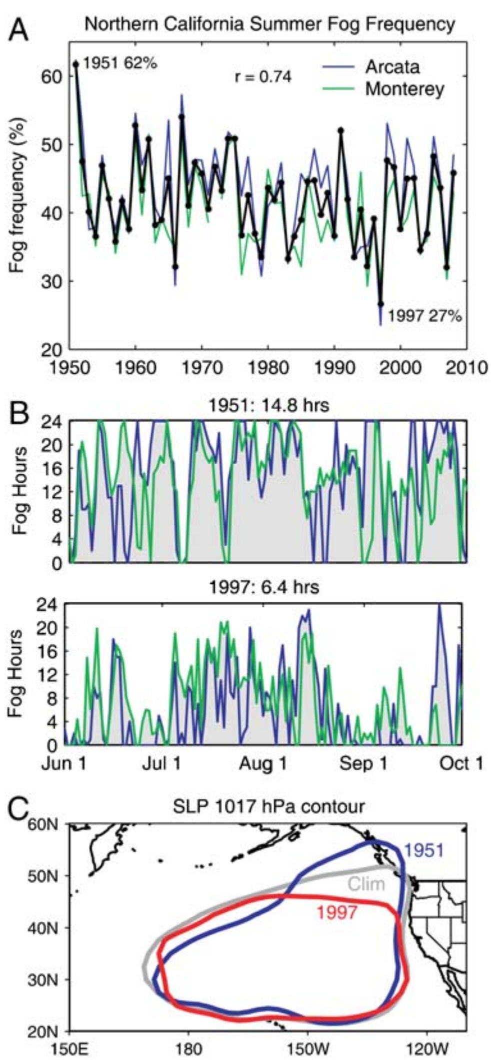

Fig. 2. Interannual variability of northern California summer fog, 1951–2008. (*A*) Summer fog frequency. Northern California index in black. (*B*) Daily fog during maximum (1951) and minimum (1997) summers. (*C*) SLP 1017 hPa isobar, illustrating the North Pacific High in 1951 (*Blue*), 1997 (*Red*), and its climatological average (*Gray*).

Interannual correlations between northern California summer fog frequency and SLP (Fig. 3*A*) are strongest off the Washington coast (maximum $r = 0.56$ at 47.5°N, 132.5°W), showing a systematic relationship to the NE-ward extent of the North Pacific High, as seen in the extreme cases. Negative SLP-fog correlations occur to the south and east of coastal northern California, covering much of SW North America. Pressure correlations over land are weak compared to those over the ocean, suggesting that Pacific atmospheric patterns are the more important control on interannual variability.

Consistent with its regional pressure signature, northern California fog also correlates strongly with the northerly wind speed along the NW U.S. coast (maximum $r = 0.69$ at 45°N, 125°W) (Fig. 3*B*). On both interannual and interdecadal time scales, a coupling is thus apparent between upwelling-favorable conditions over the California Current and the frequency of coastal fog in northern California. The atmospheric conditions that enhance nutrient supply in the surface ocean via upwelling may provide similar benefits to coastal forests via wet deposition of nitrogen in fog water, as observed in California coast redwoods (7) and in Chile (32, 33).

Northern California summer fog also displays significant connections to sea-surface temperature (SST) anomalies over much of the North Pacific basin (Fig. 3*C*). Fog enhancement occurs in association with cool ocean conditions along the west coast of North America from Alaska to Mexico, with the strongest correlation observed at the Oregon–California border (minimum $r = -0.62$ at 42°N, 124°W). Contrasting positive correlations are seen over the central and western North Pacific. This spatial pattern matches the essential form of the Pacific Decadal Oscillation (PDO), defined by the leading mode of North Pacific SST variability, after removal of the global mean (34). The 20th century PDO record shows evidence of step-like shifts associated with fish population changes in the coastal waters of western North America (34). Summer fog and PDO time series ($r = -0.52$) (Fig. 3*D*) display similar patterns of low-frequency variability, including shifts toward higher coastal SST and reduced fog frequency in the mid-1970s, as previously noted for fog in southern California (31). The summer PDO, like fog frequency, shows evidence of reversion to 1951–1976 values beginning in 1998.

Because northern California coastal fog displays strong diurnal variations and a complex pattern of inland penetration, to the casual observer it may appear to be a patchy, irregular phenomenon. Analysis of long-term records, however, reveals summer fog to be a regionally coherent climatic element on interannual to multidecadal time scales, with systematic coupling to the broader ocean-atmosphere system of the NE Pacific, including the North Pacific High, upwelling-favorable winds, and the PDO (Fig. S3).

Fog and Coastal Climate over Land. In order to determine relationships with coastal temperatures over land in three dimensions, summer fog frequency was compared to upper-air temperatures measured at Oakland (CA) International Airport (37.8°N) and near-surface T_{MAX} over the western U.S. from the Pacific

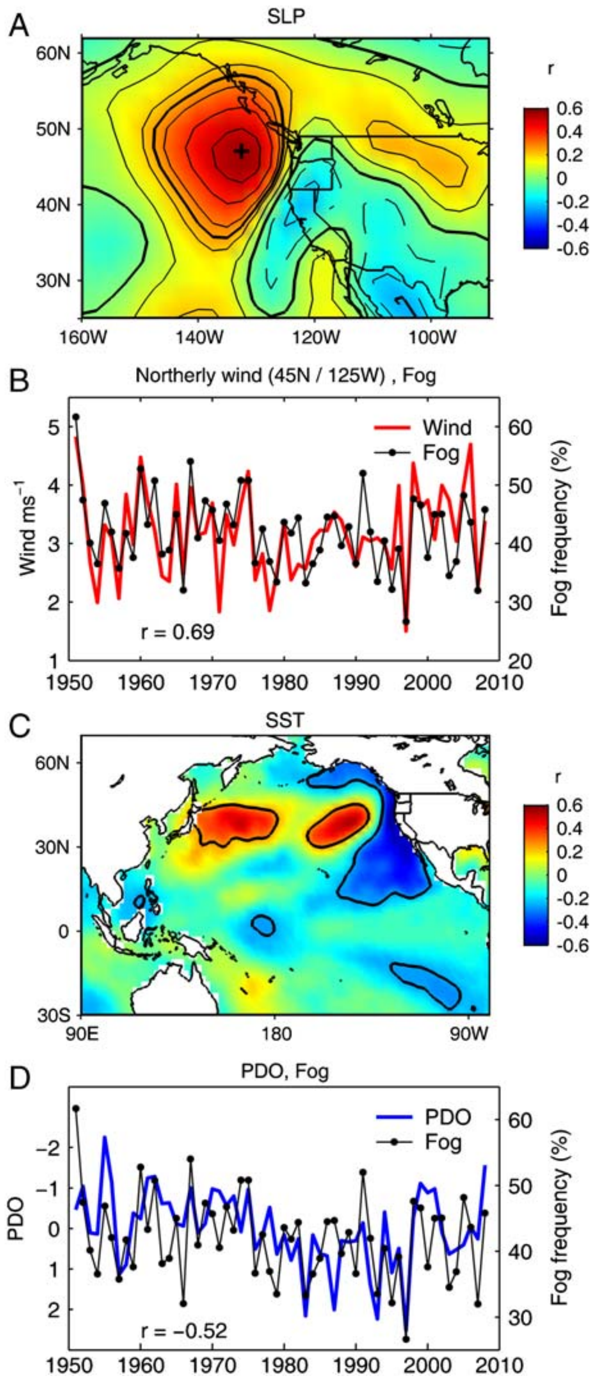

Fig. 3. Pacific climate correlations with northern California summer fog, 1951–2008. (*A*) SLP. Negative contours dashed. Bold contours mark zero line and 95% significance. (*B*) Summer fog frequency and the northerly component of 1000 hPa wind at 42°N, 124°W (Oregon–California border). (*C*) SST. Bold contours mark 95% significance. (*D*) Summer fog frequency and the PDO index of North Pacific SST.

coastline to ~300 km inland. At Oakland, vertical temperature correlations with summer fog (Fig. 4*A*) are negative within the marine layer from the surface to 400 m, reflecting cool low-level conditions during summers of increased fog (minimum $r = -0.62$ at 100 m). Above the marine layer, correlations are positive, however, peaking from 1,000–2,000 m. The summer temperature difference between these layers correlates with fog frequency at the level $r = 0.70$, reflecting a connection to the strength of the low-level coastal temperature inversion. Fog frequency was also compared to Western U.S. station records of summer T_{MAX} from the U.S. Historical Climatology Network Version 2 (USHCN v2) (see *Materials and Methods*). Uniformly negative correlations occur not just within coastal northern California but along the length of the U.S. Pacific coastline (Fig. 4*B*). East of the coastal mountain barrier, fog–T_{MAX} correlations are broadly positive, yielding a dipole signature in surface temperatures, as seen in the vertical profile.

The coast-interior contrast was identified separately in the T_{MAX} records by performing a principal components analysis of all 114 USHCN v2 station series from the region for the period from 1901 to 2008 (Fig. S4; see *Materials and Methods* and *SI Text*). The fog-related coast-interior contrast is captured by the third principal component (PC 3), which explains 10% of overall T_{MAX} variance (Figs. S4*C* and *F*). The PC 3 time series correlates strongly with both northern California fog frequency ($r = 0.84$) (Fig. 4*C*) and Oakland inversion strength ($r = 0.80$) since 1951.

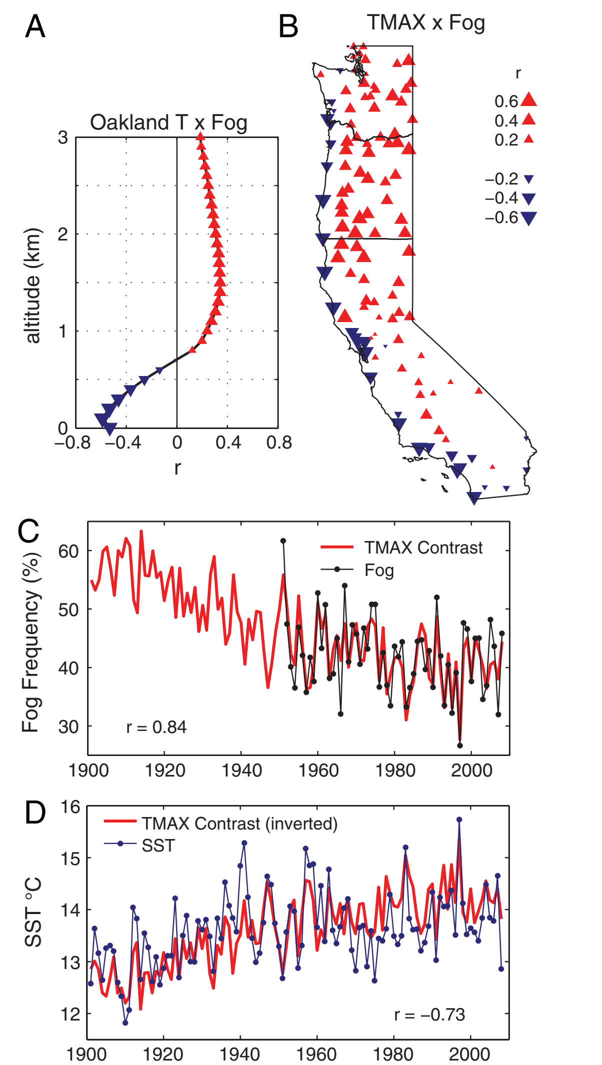

Fig. 4. Fog-temperature relationships. (*A*) Correlations: Oakland summer mean upper-air temperatures vs. northern California summer fog frequency, 1957–2008. (*B*) Correlations: Summer mean T_{MAX} vs. fog frequency, 1951–2008. (*C*) Fog frequency and T_{MAX} PC 3 (inland-coast difference), scaled as a univariate linear least-squares predictor of fog frequency, 1901–2008. (*D*) Time series comparison of T_{MAX} PC 3 and coastal SST at 42°N 124°W.

Discussion

The strong coupling of northern California coastal fog with both vertical and coast-inland temperature gradients leads to a simple conceptual model of regional summer climate variability. During summers of strong subsidence, inversion conditions, and upwelling, fog is frequent, and cool marine air and clouds tend to be sequestered at the coastline, while clear skies and compressional adiabatic warming prevail over the interior. Under lower pressure and reduced subsidence, adiabatic warming is less prevalent, the inversion is weak, and northerly upwelling winds are lessened. Fog is inhibited, and marine air passes over the coastal mountains, producing relatively warm, dry conditions along the coastline and cooler conditions inland. Such behavior in the atmosphere has long been recognized on daily time scales (35); here, we also find its clear imprint on the coastal temperature structure at annual to multidecadal scales. In this context, year-to-year changes in the coast-inland surface temperature contrast are seen mainly as a projection of inversion variability on the regional topography.

Century-Long Changes in Fog-Related Climate. The full 1901–2008 T_{MAX} PC 3 time series displays a pronounced trend, indicating a reduction in the daytime temperature contrast over the U.S. Pacific coast and suggesting decreases in fog frequency and coastal inversion strength (Fig. 4*C* and Figs. S5 and S6). By regressing the northern California fog index on T_{MAX} PC 3 (Fig. 4*C*), mean fog frequency from 1901 to 1925 is estimated at 56%, a level 33% above the observed 1951–2008 average in relative terms. Oakland inversion strength is similarly estimated to have declined from 4.1 to 1.9 °C (Fig. S6).

The temporal behavior of T_{MAX} PC 3 is closely matched by coastal SST at the Oregon–California border ($r = -0.73$ at 42° N, 124°W) (Fig. 4*D*), with both series reflecting surface warming along the coast, particularly during the first half of the 20th century. Paleoecological records from southern California Current marine sediments similarly show a post-1925 ocean warming, an anomalous feature within the past several hundred years (36). The trend in T_{MAX} PC 3 also implies greater warming at coastal than interior sites in the U.S. Pacific region (see *SI Text*).

These conclusions differ from those reached by observational (37, 38) and modeling studies (39, 40) suggesting increases in northern California coastal fog in response to enhanced greenhouse forcing. These studies have proposed that disproportionate radiative heating over interior land areas might lead to increases in the ocean-land pressure gradient and therefore stronger upwelling winds and greater fog frequency. Our results do show a strong positive relationship between northern California fog and upwelling-favorable winds over the northern limb of the California Current. However, we find direct evidence for moderate fog *reductions* since 1951, with interannual and multidecadal variations governed largely by ocean-atmosphere circulation and temperature anomalies related to the PDO. The more substantial pre-1950 decline, inferred from temperature data, may be reasonably attributed to a gradual retraction of the North Pacific High from the far NE Pacific, leading to a weakening of the temperature inversion, decreased upwelling, and low-level coastal warming.

Implications for Coastal Terrestrial Ecology. On the basis of previous research (5–7, 13, 21, 23), changes in fog frequency and related climate variables may have important implications for redwood tree physiology and ecosystem function. The effects of fog on redwood environment and transpiration are apparent in data measured at a field plot near the center of the range in Sonoma County, CA, illustrated for the period from June 7 to 18, 2003 (Fig. 5). Observations come from the Grove of the Old Trees, a ridgetop redwood preserve at 300 m elevation just west of Occidental, CA (38.40°N, 122.99°W), 8 km from the Pacific Ocean. Fig. 5*A* shows the hourly evolution of trunk-level redwood sap flow velocity (water use) and leaf wetness (the accumulation of water on leaf surfaces), as well as the ambient atmospheric vapor pressure deficit (VPD), a measure of the atmospheric demand for water from leaves. Fig. 5*B* illustrates the simultaneous variability of hourly cloud height at Sonoma County airport, located ~17 km inland. As shown by previous studies (5, 7) the presence of low clouds sharply reduces forest VPD and redwood transpiration during day and night. Here, we also find close agreement between tree-level transpiration and nearby airport cloud levels. Sap flow rates under low clouds (June 7–11) reached only 26% of those observed under clear skies (June 12–17). By reducing transpiration rates, low clouds provide an atmospheric mechanism for redwood water conservation during the dry summer season. The most likely effect of fog decline is a heightened drought sensitivity for coastally restricted plants (8). Fog is clearly a dominant climatic factor on the California coast, and long-term reductions likely have and may continue to impact the water and carbon economy of redwoods and other coastal endemic species. Prior tree-ring studies have noted significant positive correlations between summer fog frequency and the annual growth of endemic coastal California pines (12, 41). Ongoing redwood tree-ring analysis, investigating both growth rates and stable isotope signatures, may further elucidate the recent and distant history of California coastal climate and redwood responses.

Materials and Methods

The primary data consist of hourly cloud ceiling height measurements in the U.S. Surface Airways dataset, obtained from the National Climatic Data Center (NCDC). The cloud ceiling is defined as "the height above ground level of the lowest cloud or obscuring phenomena layer aloft with 5/8 or more summation total sky cover, which may be predominantly opaque, or the vertical visibility into a surface-based obstruction" (42). The northern California fog frequency index was calculated as the mean of Arcata and Monterey summer values, after converting hourly records to daily averages. Cloud data consist of measurements taken by airport observers and, over the past decade, increasingly by automated laser ceilometers (42). The Monterey site (currently Monterey Peninsula, formerly Monterey Naval Air Facility)

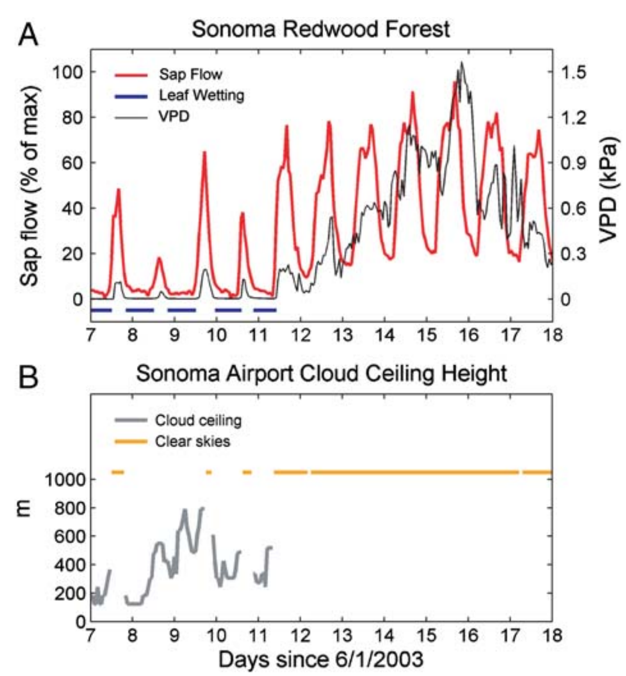

Fig. 5. Effects of fog on redwood environment and physiology. (*A*) Hourly standardized sap flow, leaf wetness, and atmospheric saturation VPD within a redwood forest in Sonoma County, CA, 8 km from the ocean, June 7–18, 2003. (*B*) Cloud height measured over the same period at Sonoma County Airport, ~17 km inland from the field site.

underwent a minor (<2 km) relocation in 1999. Each site is located within 3 km of the Pacific, with similar elevation and unobstructed N-NW exposure. During certain intervals, nighttime (2300-0500 local time) measurements are missing (Monterey 1951–57, 1965–72, 1982–1997) or taken at 3-hour resolution (Arcata 1965–72). Missing hourly summer means were infilled by creating separate hourly summer time series for each station and regressing missing data from available hourly series. Data are missing entirely at Monterey in 1973 and were filled by linear regression against the Arcata series.

SLP and wind data were obtained from the monthly 2.5°-gridded National Centers for Environmental Prediction–National Center for Atmospheric Research Reanalysis, obtained from Columbia University http://ingrid.ldeo.columbia.edu/. SST data come from the National Oceanic and Atmospheric Administration Extended Reconstructed SST dataset, version 3b (43), gridded at 2° resolution (http://www.cdc.noaa.gov/data/gridded/data.noaa.ersst.html). USHCN v2 monthly T_{MAX} averages were obtained from the NCDC http://www.ncdc.noaa.gov/oa/climate/research/ushcn/ (44). This dataset is a subset of National Weather Service Cooperative station records, selected for length and measurement consistency. USHCN v2 station data have undergone substantial correction and infilling procedures, many of which are comparable in magnitude to the observed trends. To emphasize common large-scale patterns in the data, principal components analysis was performed, by using the correlation matrix of all 114 stations in the spatial domain under consideration.

Oakland upper-air data were obtained online from the NCDC http://www.ncdc.noaa.gov/oa/upperair.html, and converted to 0000 and 1200 UTC time averages, interpolated to 100 m vertical resolution. SST averages (1971–2000) in Fig. 1 were obtained from the Reynolds and Smith 1° optimally interpolated SST climatology (version 2) (45). High-resolution (30-arc-second) land T_{MAX} averages over the same interval come from the PRISM Climate Group, Oregon State University, http://www.prismclimate.org, obtained February 19, 2009. Topographic data at the same resolution were obtained from the National Geophysical Data Center, http://www.ngdc.noaa.gov/mgg/topo/state.html, and coast redwood distribution data were obtained from the U.S. Geological Survey, http://esp.cr.usgs.gov/data/atlas/little/. The monthly PDO index was obtained from University of Washington, http://jisao.washington.edu/pdo/PDO.latest. The satellite image in Fig. 1 was obtained online from the Naval Research Lab at Monterey, CA, http://www.nrlmry.navy.mil/sat-bin/epac_westcoast.cgi.

ACKNOWLEDGMENTS. We appreciate particularly useful discussions with John Chiang, John Roden, Anthony Ambrose, Kathleen Weathers, John M. Wallace, and the input of one anonymous reviewer, which led to improvements in the manuscript. We also thank the Save the Redwoods League and the Berkeley Atmospheric Sciences Center for financial support.

1. Mann KH, Lazier JRN (1996) *Dynamics of Marine Ecosystems: Biological-Physical Interactions in the Oceans* (Blackwell Science, Cambridge, MA).
2. Garreaud R, Barichivich J, Christie DA, Maldonado A (2008) Interannual variability of the coastal fog at Fray Jorge relict forests in semiarid Chile. *J Geophys Res* 113:G04011.
3. Leipper DF (1995) Fog forecasting objectively in the California coastal area using LIBS. *Weather Forecast* 10:741–762.
4. Azevedo J, Morgan DL (1974) Fog precipitation in coastal California forests. *Ecology* 55(5):1135–1141.
5. Burgess SSO, Dawson TE (2004) The contribution of fog to the water relations of Sequoia sempervirens (D. Don): Foliar uptake and prevention of dehydration. *Plant Cell Environ* 27(8):1023–1034.
6. Dawson TE (1998) Fog in the California redwood forest: Ecosystem inputs and use by plants. *Oecologia* 117(4):476–485.
7. Ewing HA, et al. (2009) Fog water and ecosystem function: Heterogeneity in a California redwood forest. *Ecosystems* 12:417–433.
8. Fischer DT, Still CJ, Williams AP (2009) Significance of summer fog and overcast for drought stress and ecological functioning of coastal California endemic plant species. *J Biogeogr* 36:783–799.
9. Ingraham NL, Matthews RA (1995) The importance of fog-drip water to vegetation—Point Reyes peninsula, California. *J Hydrol* 164(1–4):269–285.
10. Oberlander GT (1956) Summer fog precipitation on the San Francisco peninsula. *Ecology* 37(4):851–852.
11. Weathers KC (1999) The importance of cloud and fog in the maintenance of ecosystems. *Trends Ecol Evol* 14(6):214–215.
12. Williams AP, Still CJ, Fischer DT, Leavitt SL (2008) The influence of summertime fog and overcast clouds on the growth of a coastal California pine: A tree-ring study. *Oecologia* 156:601–611.
13. Corbin JD, Thomsen MA, Dawson TE, D'Antonio CM (2005) Summer water use by California coastal prairie grasses: Fog, drought, and community composition. *Oecologia* 145(4):511–521.
14. del-Val E, et al. (2006) Rain forest islands in the Chilean semiarid region: Fog-dependency, ecosystem persistence and tree regeneration. *Ecosystems* 9:598–608.
15. (2000) *The Redwood Forest: History, Ecology and Conservation of the Coast Redwoods*, ed Noss R (Island Press, Washington, DC).
16. Florin R (1963) The distribution of conifer and taxad genera in time and space. *Acta Horti Bergiani* 20:121–312.
17. Barron JA, Heusser L, Herbert TD, Lyle M (2003) High-resolution climatic evolution of coastal northern California during the past 16,000 years. *Paleoceanography* 18(1):20-1–20-19.
18. Heusser L (1998) Direct correlation of millenial-scale changes in western North American vegetation and climate with changes in the California Current system over the past ~60 kyr. *Paleoceanography* 13(3):252–262.
19. Herbert TD, et al. (2001) Collapse of the California Current during glacial maxima linked to climate change on land. *Science* 293:71–76.
20. Ortiz J, Mix A (1997) The California Current of the last glacial maximum: Reconstruction at 42°N based on multiple proxies. *Paleoceanography* 12(2):191–205.
21. Simonin KS, Santiago LS, Dawson TE (2009) Fog interception by *Sequoia sempervirens* (D. Don) crowns decouples physiology from soil water deficit. *Plant Cell Environ* 32:882–892.
22. Parsons JJ (1960) "Fog drip" from coastal stratus, with special reference to California. *Weather* 15:58–62.
23. Limm EB, Simonin KS, Bothman AG, Dawson TE (2009) Foliar water uptake: A common water acquisition strategy for plants of the redwood forest. *Oecologia* 161:449–459.
24. Roden JS, Johnstone JA, Dawson TE (2009) Intra-annual variation in the stable oxygen and carbon isotope ratios of cellulose in tree rings of coast redwood (Sequoia sempervirens). *Holocene* 19(1):189–197.
25. Taylor SV, Cayan DR, Graham NE, Georgakakos KP (2008) Northerly surface winds over the eastern North Pacific Ocean in spring and summer. *J Geophys Res* 113(D2):D02110.
26. Koračin D, Businger J, Dorman C, Lewis J (2005) Formation, evolution, and dissipation of coastal sea fog. *Bound-Lay Meteorol* 117(3):447–478.
27. Leipper DF (1994) Fog on the U.S. west coast: A review. *Bull Am Meterol Soc* 75(2):229–240.
28. Lewis J, Koračin D, Rabin R, Businger J (2003) Sea fog off the California coast: Viewed in the context of transient weather systems. *J Geophys Res* 108(D15):6-1–6-17.
29. Pilié RJ, Mack EJ, Rogers CW, Katz U, Kocmond WC (1979) Formation of marine fog and the development of fog-stratus systems along the California coast. *J Appl Meteorol* 18(10):1275–1286.
30. Filonczuk MK, Cayan DR, Riddle LG (1995) Variability of marine fog along the California coast. *SIO Reference No 95-2* (Scripps Inst of Oceanography, La Jolla, CA).
31. Witiw MR, LaDochy S (2008) Trends in fog frequencies in the Los Angeles Basin. *Atmos Res* 87(3–4):293–300.
32. Oyarzún CE, Godoy R, De Schrijver A, Staelens J, Lust N (2004) Water chemistry and nutrient budgets in an undisturbed evergreeen rainforest of southern Chile. *Biogeochemistry* 71(1):107–123.
33. Weathers KC, Lovett GM, Likens GE, Caraco NFM (2000) Inputs of nitrogen to forest ecosystems in southern Chile: Forms, fluxes, and sources. *Ecosystems* 3(6):590–595.
34. Mantua NJ, Hare SR, Zhang Y, Wallace JM, Francis RC (1997) A Pacific interdecadal climate oscillation with impacts on salmon production. *Bull Am Meterol Soc* 78(6):1069–1079.
35. Fosberg MA, Schroeder MJ (1966) Marine air penetration in central California. *J Appl Meteorol* 5(5):573–589.
36. Field DB, Baumgartner TR, Charles CD, Ferreira-Bartrina V, Ohman MD (2006) Planktonic foraminifera of the California Current reflect 20th century warming. *Science* 311:63–66.
37. Bakun A (1990) Global climate change and intensification of coastal ocean upwelling. *Science* 247(4939):198–201.
38. Lebassi B, et al. (2009) Observed 1970–2005 cooling of summer daytime temperatures in coastal California. *J Climate* 22(13):3558–3573.
39. Diffenbaugh NS, Snyder MA, Sloan LC (2004) Could CO_2-induced land-cover feedbacks alter near-shore upwelling regimes?. *Proc Natl Acad Sci USA* 101(1):27–32.
40. Snyder MA, Sloan LC, Diffenbaugh NS, Bell JS (2003) Future climate change and upwelling in the California Current. *Geophys Res Lett* 30(15):8-1–8-4.
41. Biondi F, Cayan DR, Berger WH (1997) Dendroclimatology of Torrey pine (*Pinus torreyana* Parry ex Carr.). *Am Midl Nat* 138(2):237–251.
42. NCDC (2008) Federal Climate Complex Data Documentation for Integrated Surface Data. (Air Force Combat Climatology Center, Asheville, NC).
43. Smith TM, Reynolds RW, Peterson TC, Lawrimore J (2008) Improvements to NOAA's Historical Merged Land-Ocean Surface Temperature Analysis (1880–2006). *J Climate* 21(10):2283–2296.
44. Menne MJ, Williams CN, Vose RS (2009) The United States Historical Climatology Network monthly temperature data—Version 2. *Bull Am Meterol Soc* 90(7):993–1007.
45. Reynolds RW, Rayner NA, Smith TM, Stokes DC, Wang W (2002) An improved in situ and satellite SST analysis for climate. *J Climate* 15:1609–1625.